Development 122, 2661-2672 (1996)
Printed in Great Britain © The Company of Biologists Limited 1996
DEV1100

CSF-1 deficiency in mice results in abnormal brain development

M. Dror Michaelson[1], Phyllis L. Bieri[2], Mark F. Mehler[1,2], Hong Xu[1], Joseph C. Arezzo[1], Jeffrey W. Pollard[3,4] and John A. Kessler[1,2,*]

Departments of [1]Neuroscience, [2]Neurology, [3]Developmental and Molecular Biology, and [4]Obstetrics and Gynecology, Albert Einstein College of Medicine, 330 Kennedy Center, 1300 Morris Park Avenue, Bronx, NY 10461, USA

*Author for correspondence (e-mail: kessler@aecom.yu.edu)

SUMMARY

Colony stimulating factor-1 (CSF-1) was initially identified as a growth factor for mononuclear phagocytes. This study examines the role of CSF-1 in the development of the central nervous system (CNS). CSF-1 treatment of neurons cultured from embryonic brain promoted survival and process outgrowth in a dose-dependent manner. By contrast, CSF-1 treatment of neurons cultured from the osteopetrotic (*op/op)* mouse, a null mutant for CSF-1, promoted significantly less process outgrowth, suggesting that there are neural abnormalities in *op/op* animals. Nuclease protection assays were used to determine whether CSF-1 and its receptor are expressed at times appropriate to regulate neural development. Both CSF-1 and its receptor are expressed in developing mouse brain, with a unique pattern of CSF-1 mRNA splice variant expression encoding secreted, and not membrane-bound, growth factor. To determine whether brain function is altered by null mutation of CSF-1, *op/op* mice were examined using electrophysiologic assays. Brainstem auditory and visual evoked potentials were both abnormal in *op/op* mice. Further, intracortical recordings revealed aberrant neuronal function within visual cortex and alterations in the cortical circuitry that balances excitation and inhibition. Daily CSF-1 injection of postnatal *op/op* mice largely rescued the abnormal neural phenotype, confirming that the absence of CSF-1 during development is responsible for the abnormalities. The effects of CSF-1 on cultured embryonic neural cells, the developmentally appropriate expression of CSF-1 and its receptor, and the neurological abnormalities in *op*/*op* mice suggest a role for CSF-1 in brain development.

Key words: CSF-1, colony stimulating factor, brain, *op*/*op* mice, osteopetrotic, CNS development, neurotrophic factor, evoked potential, mouse

INTRODUCTION

CSF-1 is a growth factor that regulates the survival, proliferation and differentiation of the mononuclear phagocyte lineage (Stanley et al., 1983). CSF-1 is also likely to be an important factor in placental regulation and maternal/fetal interactions (Pollard et al., 1987; Arceci et al., 1989; Regenstreif and Rossant, 1989). The importance of CSF-1 in both the regulation of the mononuclear phagocyte lineage and in fertility has been convincingly demonstrated by studies with the CSF-1 null mutant osteopetrotic (*op*/*op*) mouse (Pollard and Stanley, 1996). A single basepair insertion generates a stop codon approximately 280 basepairs into the coding region of the CSF-1 gene (now referred to as *csf-m^{op}*), and homozygous mutant mice totally lack functional CSF-1 (Yoshida et al., 1990; Wiktor-Jedrzejczak et al., 1990; Pollard et al., 1991). The *op/op* mouse has impaired bone remodeling due to an absence of osteoclasts, resulting in osteopetrosis (Marks and Lane, 1976; Wiktor-Jedrzejczak et al., 1982, 1990, 1991; Kodama et al., 1991). This phenotype can be corrected by injections of recombinant CSF-1 (Kodama et al., 1991; Wiktor-Jedrzejczak et al., 1991). Retarded skeletal growth and excessive accumulation of bone are ordinarily observed until about 2 months postnatally, after which the defects gradually disappear (Begg et al., 1993; Marks and Lane, 1976). Analysis of the macrophage/monocyte lineages in *op/op* mice reveals that certain populations of phagocytes are particularly depleted, such as macrophages of the spleen marginal zone, liver, kidney and gut, whereas other populations, such as lymph node macrophages, are relatively intact (Wiktor-Jedrzejczak et al., 1991; Witmer-Pack et al., 1993; Cecchini et al., 1994).

The gene encoding CSF-1 in both the human and mouse spans 21 kilobases (kb) and consists of 10 distinct exons, the first eight of which contain peptide-coding sequences. Differential splicing within exon 6 generates soluble or membrane-bound forms of CSF-1, which differ in speed of proteolytic cleavage and subsequent release from the cell. Additionally, splicing in the 3′ non-coding region joins either exon 9 or exon 10, but not both, to exons 1-8 (for reviews, see Kawasaki and Ladner, 1990; Roth and Stanley, 1992; Pollard and Stanley, 1995). Post-translationally, CSF-1 is glycosylated in the endoplasmic reticulum and the Golgi apparatus, and the predominant secreted form of CSF-1 is a proteoglycan (Price et al., 1992). CSF-1 mRNA is expressed in vitro by endothelial cells,

fibroblasts, marrow stromal cells and brain astrocytes, as well as uterine epithelial cells from pregnant animals (Pollard et al., 1987; Daiter et al., 1992; Roth and Stanley, 1992).

The biological activity of CSF-1 is mediated by a single high-affinity cell-surface receptor, encoded by the c-*fms* protooncogene, which belongs to the class III family of intrinsic tyrosine kinase growth factor receptors. The CSF-1 receptor (CSF-1R) is expressed predominantly on mononuclear phagocytes, with lower densities of surface expression on multipotent stem cells in the hematopoietic lineage. Both CSF-1 and its receptor are expressed at high levels in the uteroplacental unit (Arceci, 1989; Regenstreif and Rossant, 1989; Daiter et al., 1992; Pampfer et al., 1992). Additional cell types have been shown to express CSF-1R, including the macrophage-like microglial cells in the nervous system (Sawada et al., 1990; Brosnan et al., 1993).

Observations of *op*/*op* mice in a free-field cage setting suggest that they have some sensory deficits, since they do not respond appropriately to external cues. The brains of *op/op* mice are grossly normal, with unremarkable cytoarchitecture, and microglia appear to be normal in the adult (Chang et al., 1994). However, analysis of *op/op* neural function reveals severe deficits, including impaired auditory and visual processing, with specific abnormalities within the cerebral cortex. Additionally, CSF-1 enhances process outgrowth and survival of neurons cultured from embryonic brain of normal mice, but there is significantly less process extension from *op/op* neurons in culture. CSF-1 and CSF-1R mRNA are expressed in vivo in various regions of developing brain. The neurotrophic effects of CSF-1 treatment and the expression of the factor in developing brain provide a background for understanding the CNS pathophysiology in *op*/*op* mice; taken together, these findings suggest that CSF-1 is an important trophic factor in brain development.

MATERIALS AND METHODS

Animals

Osteopetrotic *op/op* mice and littermate controls were bred and maintained as previously described at the Albert Einstein College of Medicine animal house (Pollard et al., 1991). Mice were fed ad libitum with powdered chow and infant milk formula. Homozygote *op/op* mutants were distinguished from phenotypically normal littermates based on the absence of incisors and by a domed skull (Marks and Lane, 1976). Normal +/+ were distinguished from heterozygous +/*op* by an allele-specific PCR-based assay (Cohen et al, 1996). Electrophysiological studies were performed on 9- to 12-week-old mice. In reconstitution experiments, animals were injected subcutaneously on a daily basis for 10 weeks, starting on postnatal day 2, with either saline or CSF-1 (a generous gift of Chiron Corporation) at 1 million units/day (1 unit = 12 pg protein).

Electrophysiology

Extracranial electrophysiology was obtained in 13 mice (6 *op/op* and 7 littermate controls). Measurements included brainstem auditory evoked potentials (BAEPs) and cortical visual evoked potentials (VEPs). Animals were lightly anesthetized with halothane, respiration rate was monitored and temperature was maintained within physiologic limits. A single platinum-iridium needle electrode was positioned subcutaneously overlying lambda and referenced to the mastoid process. Auditory stimuli were approximately 90 dB clicks (50 ms square wave pulse) delivered binaurally at a rate of 5 per second through an open-field speaker. 500 stimuli were averaged for each BAEP. Neuroelectric signals were coupled via unity gain preamplifiers to Grass P5 amplifiers (6 dB down, roll-off 6 dB/octave) set at a gain of 10,000 and a bandpass of 10 Hz to 10 kHz. The amplifier outputs were digitized at 20 kHz and averaged using a Nicolet Pathfinder minicomputer. Visual stimuli were full-field, stroboscopic flashes (7.8×10^5 lux) presented in an electrically shielded, sound-attenuated and darkened chamber. Stimuli were grouped into blocks of 100 flashes and presented at a rate of 2 per second. All conditions were repeated a minimum of 4 times per subject. Intracortical electrophysiologic data were recorded in 12 mice (6 controls and 6 *op/op*). Subjects were anesthetized with ketamine (50 mg/kg, I.P.) and xylazine (40 mg/kg, I.P.), and placed in a sterotaxic instrument. The skin was resected and a small burr hole was drilled through the skull overlying primary visual cortex. A single multicontact electrode was introduced into visual cortex and positioned using an externally mounted microdrive. Data were recorded from an array of 14 equally spaced contacts, with intercontact spacings of 100 μm and impedances of approximately 300 kΩ at 1000 Hz. Stimuli were identical to those used for extracranial recording.

For select experiments, the standard multicontact electrode was fitted with a 33-gauge tapered tube to deliver microinjections of 0.5 mM bicuculline methiodide intracortically. Approximately 0.2 μl of bicuculline was injected in visual cortex of wild-type or *op/op* mice. The intracortical depth of injection was selected to correspond to lamina 4 on the basis of on-line electrophysiology.

VEPs were obtained simultaneously from multiple cortical laminae. The center of the electrode array was positioned to straddle the dipole of the initial cortical depolarization. Recording gain was set at 2,000 with a bandpass of 3 Hz to 3 kHz; signals were digitized at 2 kHz and averaged using a Nicolet Pathfinder minicomputer. Multiple unit activity was recorded and averaged in parallel with the field potentials. The amplified signal was high pass filtered above 500 Hz (roll-off 24 dB/octave), full-wave rectified, and then further amplified (gain = 8) and digitized at 4 kHz. One-dimensional current source density (CSD) analyses of the VEP profiles were calculated using a three-point formula for approximation of the second spatial derivative (Freeman and Nicholson, 1975):

$$D = \frac{\delta^2\phi}{\delta x^2} = \frac{-[\phi(x\text{-}h)-2\phi(x)+\phi(x+h)]}{h^2}$$

where 'ϕ' is the voltage, 'x' is the point at which D is calculated and 'h' is the intercontact spacing on the electrode. To further clarify the temporal aspects of current flow, CSD wave forms from multiple sites in a single cortical penetration were zeroed with respect to a prestimulus epoch, full-wave rectified and averaged. Rectification eliminates information regarding the direction of transmembrane current flow, while averaging results in loss of spatial data; however, the resulting wave form provides a simplified and accurate measure of the temporal pattern and relative magnitude of transmembrane current flow within the area sampled (Givre et al., 1994).

For the final electrophysiologic procedure, eight *op/op* mice were injected subcutaneously with CSF-1 or saline daily for 10 weeks starting on postnatal day 2. The laminar patterns of VEP, MUA and CSD were examined at 10-11 weeks. Data were scored blindly and independently by two observers (P. B. and J. A.) with respect to total pattern of current flow, timing and pattern of laminar inversion, and integrity and temporal persistence of MUA. The neural patterns were qualitatively assessed as normal or mildly, moderately or severely abnormal.

Tissue culture

Embryonic day 17 Sprague-Dawley rats were killed and brain regions immediately removed by dissection. The various regions, including hippocampus, cerebellum, cortex and hypothalamus, were incubated in trypsin at 37°C for 15 minutes and then mechanically dissociated.

24-well plates were coated with 50 μg/ml poly-D-lysine, and the cells were plated in serum-free DME medium supplemented with B-27 (Gibco), at an initial density of 10^4 cells/well. CSF-1 was added at the time of plating at a concentration that gave maximal response by dose-response analysis. Human CSF-1 was supplied by Genetics Institute (Cambridge, MA). On day 5 after plating, cultures were evaluated for survival and process outgrowth (greater than 1.5 somatic diameters). Cell counts were made from a representative area of each well.

Homozygous and heterozygous mutant mouse embryos were produced by mating *op*/+ females with *op/op* males. Cerebral cortex was dissected on embryonic day 16, and the remainder of each embryo was frozen for subsequent PCR analysis to genotype each embryo. Cortex was also dissected from E16 wild-type embryos. Each cortex was individually incubated in trypsin for 15 minutes and then mechanically dissociated. 10^4 cells per well were plated into each of two wells in serum-free DME medium supplemented with B-27 on 24-well plates coated with 50 μg/ml poly-D-lysine. One well for each animal was treated with CSF-1 at the time of plating (10 ng/ml) and the other was treated with saline. Cells were counted after 8 hours to determine whether there were any differences among groups in adhesion of cells and daily thereafter for 4 days. Three counts from different areas of each well were averaged at each time point (2.5% of the total area). On day 4, the length of the longest neurite on each cell and the number of branch points were measured using an ocular grid, for 100 cells in each well. At day 4 the cells were processed for neurofilament immunohistochemistry. A few wells were maintained for 8 days to observe process outgrowth. Since the genotype of the animals was unknown during the entire period of data collection, the observations were blinded. After genotyping there were 10 *op/op* and 11 *op*/+ animals. 12 control (+/+) animals were used.

Immunochemistry

Staining was performed as previously described (Mehler et al., 1993). Medium was removed from the culture wells and the cells washed twice in PBS. Cells were then fixed in 4% (w/v) paraformaldehyde, blocked with 5% normal goat serum for 30 minutes, and incubated overnight with primary antibody at 4°C. The following day, incubation with biotinylated secondary antibody was carried out for 30 minutes and the wells then incubated with ABC reagent (Vector Labs). Binding was visualized using 0.5 mg/ml of diaminobenzidine (Sigma). SMI31 antibody to the mature 200×10^3 M_r phosphorylated form of neurofilament was purchased from Sternberger Monoclonals, Inc..

Solution hybridization assays

The procedures followed were those described in the RPA II Kit manual (Ambion). Briefly, 10-20 μg of total RNA were coprecipitated with antisense riboprobe, incubated overnight in 20 μl hybridization buffer at 42°C, and then digested with a combination of RNase A/T_1. Following RNase inactivation, the RNA was subjected to electrophoresis on a 1.5 mm, 5% polyacrylamide gel for 2 hours at 250 V. For a molecular weight marker, the RNA Century marker was used (Ambion). The dried gel was exposed to Kodak X-Omat film with two intensifying screens at −70°C for 1-7 days.

As a negative control in each experiment, one hybridization mix contained yeast tRNA rather than tissue RNA, and no protected species were seen in these samples. A faint band was occasionally seen in these and other samples, which comigrated with full-length probe. A sample of undigested full-length probe was run on each gel to distinguish undigested probe from protected species. The former was larger due to stretches of plasmid sequences in the probe that were not protected from RNase digestion. β-Actin probe (250 bp protected species) was included in the same hybridization mixes as the c-*fms* probe, since it was significantly shorter than c-*fms* and consequently did not interfere with c-*fms* signal visualization. In parallel, c-*fms* alone was hybridized to tissue mRNA to ensure that the c-*fms* signal was constant in the presence or absence of actin. Quantitative nuclease protection assays were performed as previously described (Ludlam et al., 1994).

Riboprobe construction

The CSF-1 and c-*fms* cDNAs were cloned into riboprobe vectors containing T7 and SP6 RNA Polymerase promoters (Promega; Invitrogen). The CSF-1 exon 9 cDNA spanned bases 1793-1987 of the published mouse CSF-1 sequence, and a 194 bp antisense template was generated by linearization with *Hin*dIII (Ladner et al., 1988). The c-*fms* 423 bp probe consisted of bases 1921-2344 and a 480 bp linear template was generated by *Hin*dIII digestion. The complete mouse c-*fms* cDNA in pGEM-2 was digested with *Nhe*I to generate the 470 bp riboprobe used in the regional analysis. After linearization, 1.0 μg of template DNA was used in the riboprobe reaction with 8 μl of [^{32}P]rUTP (3000 Ci/mmol--NEN) and 2 μl of either T7 or SP6 RNA Polymerase (Promega). The sample was subjected to electrophoresis on an 8 M urea denaturing polyacrylamide gel. The region of the gel containing full-length riboprobe was incubated in elution buffer (Ambion) overnight at 37°C. For construction of actin riboprobe, template from the RPA II kit was used, with only 1 μl of [^{32}P]rUTP, and cold rUTP added to 10 μM. T3 RNA Polymerase was used to synthesize a probe of approximately 300 bp, with a protected species of 250 bp.

Reverse transcription-polymerase chain reaction (RT-PCR)

RNA was isolated from tissue by the guanidinium thiocyanate method previously described and quantitated by absorbance at 260 nm (Chomczynski and Sacchi, 1987). To remove traces of contaminating DNA, samples were digested with RQ1 RNase-free DNase (1 U/ml; Promega). First-strand cDNA synthesis utilized MMLV reverse transcriptase (Gibco). The RT mix included 35 mM $MgCl_2$, 0.2 mM of random hexanucleotides and 0.7 mM of each deoxynucleotide, and the reaction carried out at 37°C for 90 minutes. 40-cycle PCR and Southern analysis were performed as described previously (Daiter et al., 1992). Each of five sets of primers was designed to amplify specific mRNA splice variants as follows:

Primers	Sequence	Bases	Transcript detected	Product
A. J97	5′GTCCTAGAAGAAGCTTCTGGAGAG3′	1066-1089 (exon 6)		
E42	5′GGGTGGCTGAGTTGCTGAC3′	1405-1387 (exon 6)	4.6 kb	339 bp
B. E46	5′ACCAAGAACTGCAACAAC3′	662-679 (exon 5)		
J92	5′GGTAGTGGTGGATGTTCCCATATG3′	1890-1867 (exon 10)	3.0 kb	345 bp
C. E43	5′AAGACCACCAGGAGCCAGGCTCTCC3′	1334-1358 (exon 6)		
J43	5′CATTGACAAACGAGTGTGTCC3′	1866-1847 (exon 9)	2.3 kb	532 bp
D. J51	5′GTTTGCTACCTAAAGAAGGC3′	394-413 (exon 4)		
J43	5′CATTGACAAACGAGTGTGTCC3′	1866-1847 (exon 9)	1.6 kb	589 bp
E. E55	5′CGACATGGCTGGGCTCCC3′	197-214 (exons 1-2)		
J52	5′CGCATGGTCTCATCTATTAT3′	452-433 (exon 4)	all mRNAs	255 bp

Primer selections were based on the published mouse CSF-1 sequences (Ladner et al., 1988). For each pair, the sense (upstream) primer is listed first followed by the antisense (downstream) primer. The exon(s) in which each primer is located is noted.

RESULTS

Effects of CSF-1 treatment on embryonic neural cells

To characterize possible trophic actions of CSF-1 in the CNS, the effects of CSF-1 treatment of neuronal cultures were examined. Primary cell cultures were established from four regions of embryonic rat brain and were grown in serum-free medium to partially select for neuronal cells. A sufficiently low density of cells was plated to allow only minimal survival in control, untreated cultures. Experimental cultures were treated with CSF-1 at the time of plating and no further factor was added. Cells from representative areas of each well were counted 5 days after plating. In each region - hippocampus,

cerebellum, cortex and hypothalamus - CSF-1-treated cultures contained significantly more cells than untreated cultures, from 3.4-fold in hypothalamus to 6.6-fold in hippocampus (Fig. 1A).

Even more striking was the observed difference in process outgrowth between CSF-1 and control cultures (Fig. 1B). In the controls, essentially no cells (<5%) exhibited process outgrowth. In contrast, after CSF-1 treatment, 93% of cells from cerebral cortex, and 79% of cerebellar cells, exhibited processes. Hippocampal and hypothalamic cultures manifested a smaller but highly significant amount of process outgrowth as well, with 26% and 39% of cells, respectively, exhibiting processes. Dose-response analysis revealed that different concentrations of CSF-1 gave maximal responses in different brain regions (Fig. 1C). Cerebellar cultures exhibited a dose-response profile similar to hippocampus, with maximal effect on cell number at 1.0 ng/ml, while hypothalamic cultures were comparable to cortex, with maximal effect at 10.0 ng/ml.

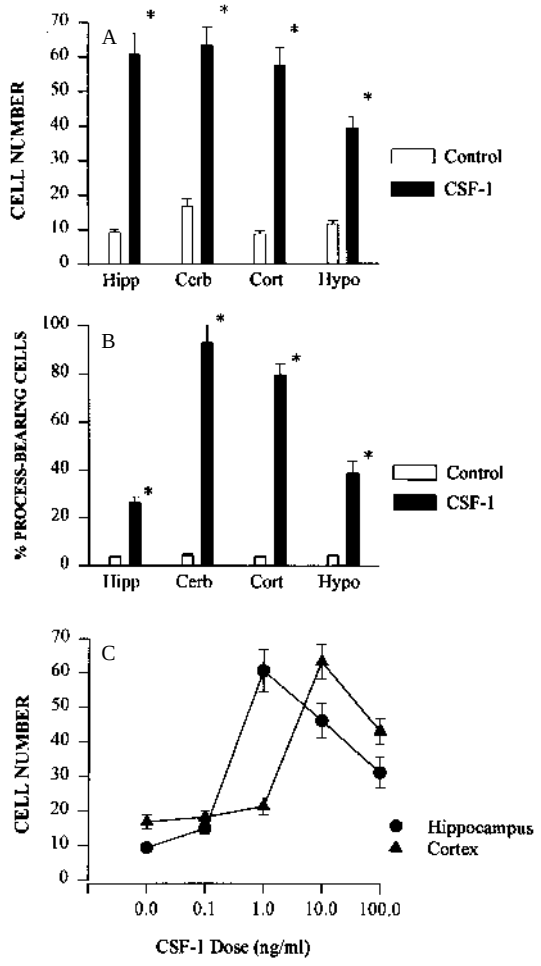

Fig. 1. Effect of CSF-1 on primary cultures from embryonic brain regions. (A) Representative areas (2.5% of total area) of wells were counted on day 5 after plating, and the average number in 8 separate wells for each sample was plotted. Hipp, hippocampus; Cerb, cerebellum; Cort, cortex; Hypo, hypothalamus. The increase in cell number in CSF-1-treated cultures was significant in each region (P<0.001). The concentration of CSF-1 added to cultures was that which gave maximal survival by dose-response: hipp-1.0 ng/ml, cerb-1.0 ng/ml, cort-10.0 ng/ml, hypo-10.0 ng/ml. (B) Cells with processes greater than 1.5 somatic diameters were counted on day 5. n=8 for each sample. Each region had significantly greater process-bearing cells after CSF-1 treatment (P<0.0001). (C) Dose-response analysis of cultured cells to CSF-1. Representative areas (2.5% of total area) of wells were counted 5 days after plating with initial indicated doses of CSF-1. The experiments in A, B and C were each repeated a minimum of five times, and error bars represent SEM.

To establish the neuronal nature of CSF-1-induced processes, cultures were stained for the mature 200×10^3 M_r form of neurofilament (NF200) on day 5 after plating (Fig. 2). Although the number of NF200-positive cells in CSF-1-treated cultures was greater than that in untreated cultures, areas containing similar cell numbers are shown in the figure in order to contrast process outgrowth. Enhancement in neurite outgrowth was particularly evident in CSF-1-treated cultures from cortex (Fig. 2B), with networks of processes extending between virtually all cells. Many hippocampal cells also displayed significant neurites (Fig. 2D), whereas control cultures from both regions had little process outgrowth (Fig. 2A,C). Cell bodies and their processes both stained for neurofilament. The significant effects of CSF-1 treatment on neuronal survival and process outgrowth begin to provide a cellular basis for CSF-1 function in normal brain development, and a rationale for examining functional interconnections of neurons in the brains of *op/op* animals.

In addition to culturing cells from normal embryonic rat brain tissue, we established neural cultures from offspring of matings of *op/op* × *op/+* mice at embryonic day 17. The cortex of each embryo from such matings was cultured separately, with corresponding tissue samples set aside for subsequent PCR genotyping. Cultures were also established from control embryos. Cultures were grown for 4 days in the presence or absence of CSF-1, and cell number and process extension were assessed daily. On day 4, complexity of processes was analyzed by measuring neurite length and the number of branch points of 100 scored neurons in each group. Following compilation of these data, genotyping was performed and the culture results were grouped accordingly. Fig. 3A demonstrates that the survival effect of CSF-1 did not differ between control or *op/op* neurons. However, significantly fewer cells manifested processes at days 1-2 in the *op/op* group (Fig. 3). Furthermore, although the percentage of cells exhibiting processes in all groups was similar by day 4, the complexity of the neurites was significantly decreased in cells cultured from *op/op* mice as compared to +/+ mice (Fig. 3D). Cultures followed to day 8 continued to demonstrate a marked difference in complexity between control and mutant cells (data not shown). In all groups, neural cells not treated with CSF-1 manifested poorer survival and process outgrowth.

Expression of CSF-1R mRNA in developing brain

To determine whether CSF-1 and its receptor are expressed at times appropriate to regulate brain development, it was important to explore the ontogeny of CSF-1 expression. CSF-1 mRNA expression in whole brain has been demonstrated (Bartocci et al., 1986; Thery et al., 1990; Burns et al., 1993; Chang et al., 1994), and we also found expression of both exon 9- and exon 10-containing transcripts in brain (data not shown). However, expression of c-*fms* mRNA, which encodes the CSF-1R, has not been extensively studied in vivo. Nuclease protection analysis was performed with antisense riboprobes complementary to the c-*fms* gene. A 420 bp riboprobe corresponding

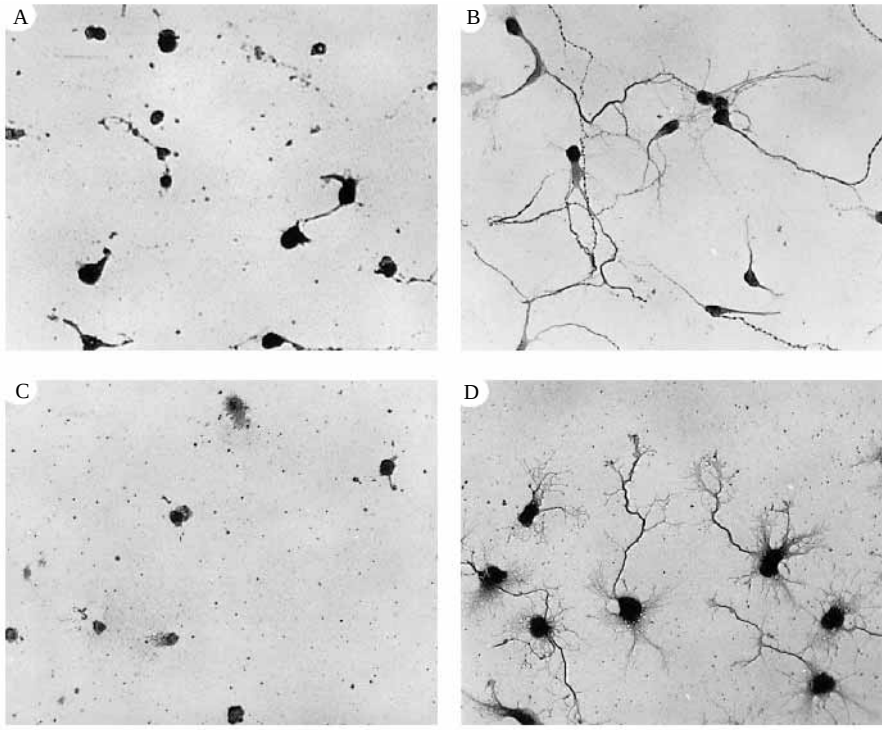

Fig. 2. Neurofilament staining of CSF-1-treated primary cultures. Cultures from both hippocampus and cerebral cortex displayed enhanced neurite outgrowth following CSF-1 treatment. Cells were stained with SMI31, an antibody to the mature 200×10^3 M_r phosphorylated form of neurofilament, 5 days after plating and treatment (200x magnification). (A) Cortex, untreated; (B) cortex, CSF-1-treated; (C) hippocampus, untreated; (D) hippocampus, CSF-1-treated.

to bases 1921-2344 of the c-*fms* cDNA detected expression in whole brain from E13 mice through adulthood (Fig. 4A). Equal loading of RNA was verified by cohybridization of each sample with a riboprobe to β-actin. To assess expression quantitatively, a standard curve was established using sense strand cRNA standards and densitometric analysis of signal strength from brain samples was performed (Fig. 4B). The level of CSF-1R mRNA increased during development until it peaked at P15 (postnatal day 15), and then declined in adult brain. Cultured neural cells were analyzed by nuclease protection analysis for expression of mRNA encoding the CSF-1R, and glial cells, but not neurons, were found to express CSF-1R mRNA (data not shown). Thus, the effects of CSF-1 on neurons are probably mediated indirectly by non-neuronal cells.

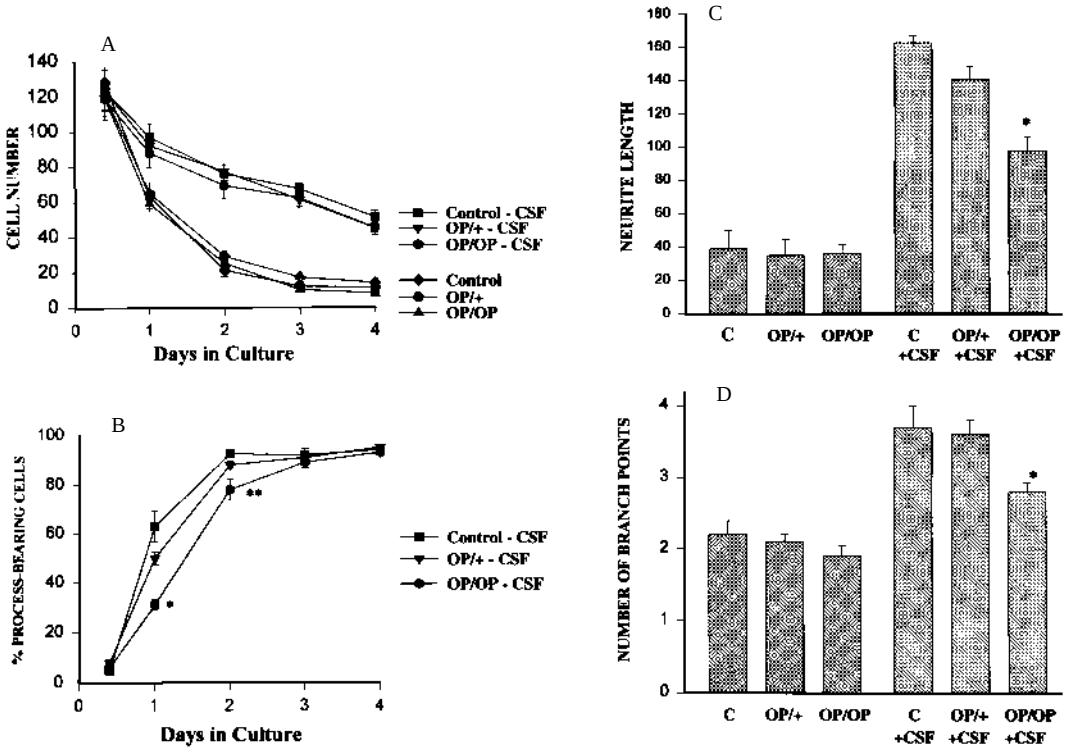

Fig. 3. Effects of CSF-1 on embryonic cerebral cortex from *op/op*, *op*/+, and +/+ mice. Cortical neurons were cultured from E16 animals either in the presence (10 ng/ml) or absence of CSF-1. (A) The number of cells was counted in each well (2.5% of total area) at 8 hours and daily thereafter for 4 days. There were no detectable differences in cell number at 8 hours indicating that CSF-1 did not alter adhesion of the cells. Values represent the mean ± SEM. (B) The cells were scored for the presence of a process at least one cell diameter in length; *, $P<0.02$ by ANOVA; **, $P<0.05$. (C,D) On day 4 the length of the longest neurite (in μm) and the number of branch points of that neurite were determined by examining 100 cells in each well using an ocular grid; *, $P<0.025$.

Regional expression of CSF-1 and CSF-1R mRNA

A regional analysis of CSF-1 mRNA expression was undertaken to identify focal areas of expression in brain, using a riboprobe complementary to exon 9 of the CSF-1 gene. In the cerebellum, levels of expression were similar in early and late development, with CSF-1 mRNA also found in the adult cerebellum (Fig. 5A). CSF-1 mRNA was present in the cerebral cortex, although the levels were considerably lower than those in cerebellum, and longer exposure times were required to detect the protected species. In hippocampus and striatum, exon 9-containing CSF-1 mRNA was not detected at any age (Fig. 5B).

A similar analysis was performed for c-*fms*. In cerebellum, cerebral cortex, hippocampus and striatum, the temporal pattern of mRNA expression reflected that of whole brain (Fig. 5A,B). Thus, in the neonate, these regions had low levels of expression, postnatal day 15 (P15) mRNA manifested higher levels of expression and the adult samples were similar to neonate (summarized in Table 1). The regional analysis was performed using a riboprobe complementary to the distal 3′ end of the c-*fms* gene, and the uppermost band protected by the probe was consistent with the expected size of 470 bp. The nature of the bands below it is unknown, but hybridization instead with the other, 420 bp riboprobe gave a single, discrete band.

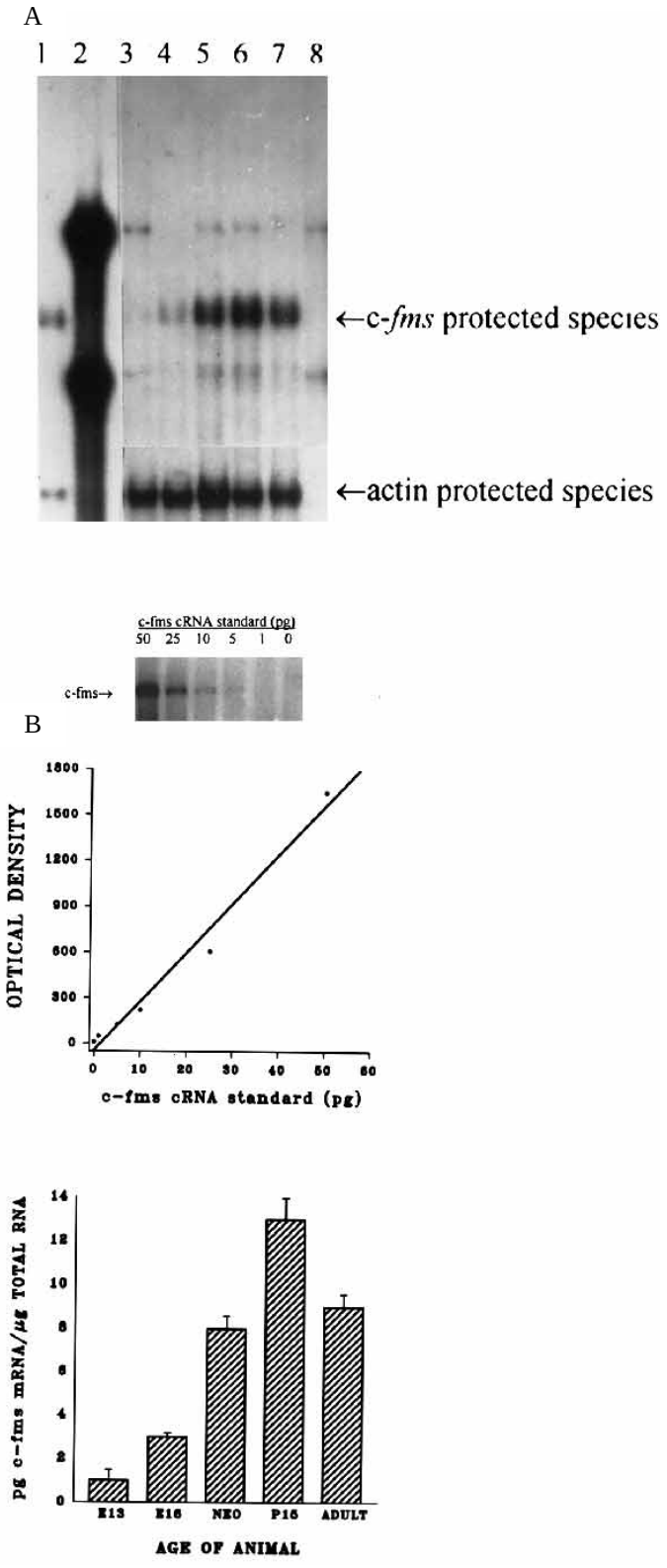

Expression of specific CSF-1 splice variants in brain

To further define CSF-1 expression in the CNS, RT-PCR analysis was utilized. Primers specific for different exons were used to elucidate which splice variants are present in brain. The four known splice variants of mouse CSF-1 mRNA are 4.6, 2.3, 3.0 and 1.6 kb (Kawasaki and Ladner, 1990). The first two contain exon 6 and differ in their 3′ untranslated region; the 4.6 kb transcript contains exon 10 and the 2.3 exon 9, respectively. The 3.0 and 1.6 kb transcripts have an alternative splice acceptor in exon 6, and differ from one another in including exon 10 or exon 9, respectively (see Table 2). In peptides encoded by transcripts containing the complete exon 6, proteolytic cleavage occurs in the secretory vesicles with subsequent rapid release from the cell. Transcripts with truncated exon 6 encode peptides that lack the secretory-vesicle-processing site and which are therefore presented at the cell surface. Thus, exon 6-containing transcripts encode the soluble

Fig. 4. (A) (top) Expression of c-*fms* mRNA in developing and adult mouse whole brain. Nuclease protection assay using mouse c-*fms* and actin antisense riboprobes with protected species of 423 and 250, respectively. Adult liver positive control, lane 1; full-length probe, lane 2 (the higher band is undigested c-*fms* probe and the lower band is undigested actin probe); E13 brain, lane 3; E16 brain, lane 4; neonate brain, lane 5; P15 brain, lane 6; adult brain, lane 7; yeast tRNA negative control, lane 8. 10 μg of total RNA were used in each sample. Levels of c-*fms* expression increase during development and peak at P15 before declining in adult brain. An exposure of 5 days is shown for the c-*fms* message; shorter exposure times are shown for the first two lanes and for actin. (B) Standard curve of c-*fms* nuclease protection assay. c-*fms* sense strand cRNA was transcribed in vitro in the presence of nonradioactive nucleotide triphosphates. Successive dilutions were then hybridized to a constant amount of antisense riboprobe and assayed by nuclease protection (top panel). Regression analysis demonstrated a linear relationship between the densitometric intensity of the bands and the amount of sense cRNA, and a representative standard curve is shown. The bottom graph is a representation of c-*fms* mRNA levels in the brain. Signal strength for c-*fms* was normalized to actin and then quantitated by comparison to the sense cRNA standards. The mean of two or three experiments, depending on the age, is shown. Levels of c-*fms* increased during development to a peak at P15 before declining in the adult. E, embryonic; neo, neonate; P, postnatal.

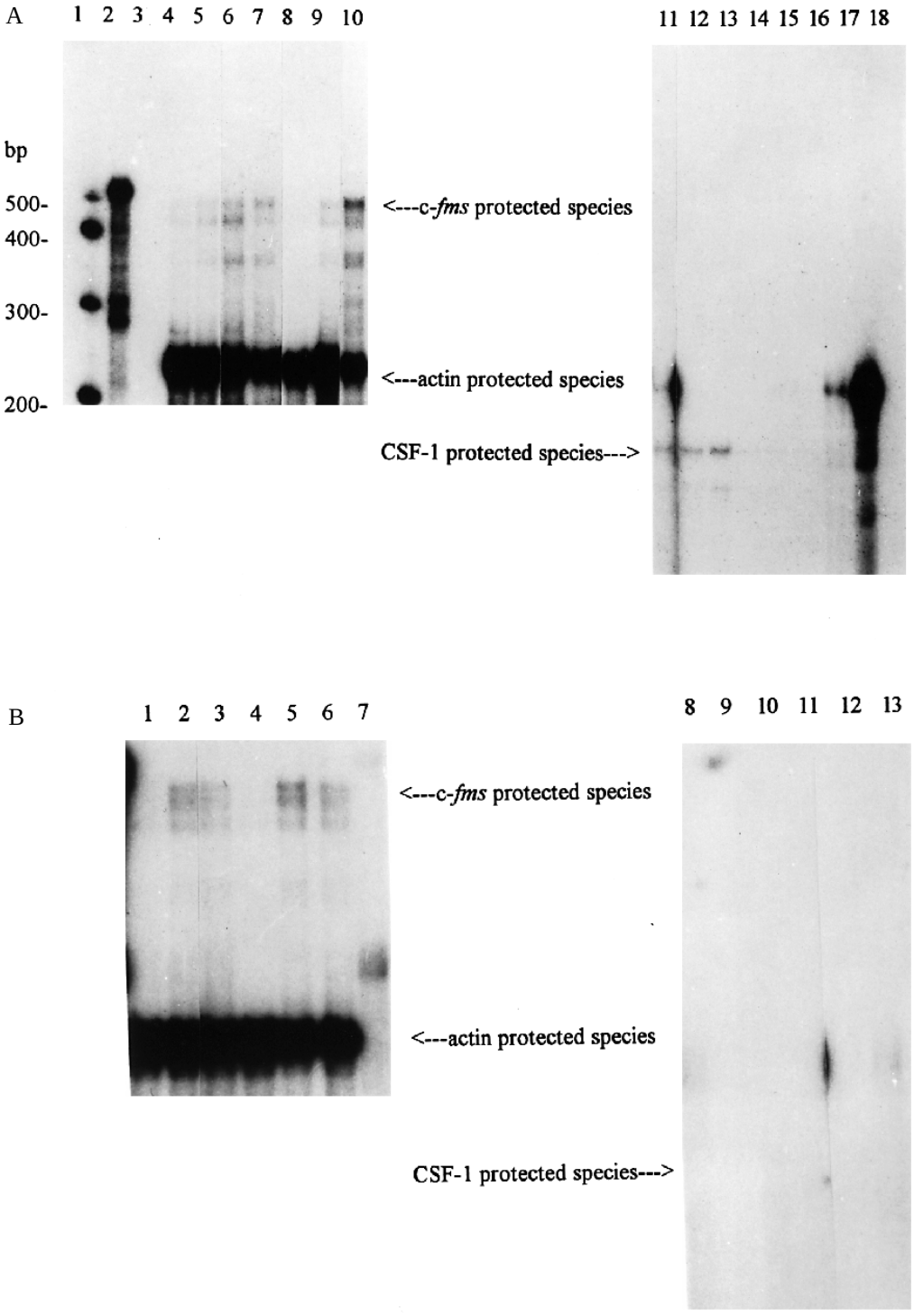

Fig. 5. Regional expression of CSF-1 and c-*fms* mRNA in developing brain. Nuclease protection assays using the CSF-1 exon 9 and the c-*fms* 423 bp riboprobes. (A) (top) Expression of c-*fms* in E16, neonate, P15, and adult cerebellum (lanes 4-7) and E16, neonate, and adult cortex (lanes 8-10); and expression of CSF-1 in E16, P15, and adult cerebellum (lanes 11-13) and E16, neonate, and adult cortex (lanes 14-16). Lane 2 contains full-length c-*fms* and actin probes, and lane 17 contains full-length CSF-1 probe. Lanes 3 and 18 are the respective yeast tRNA negative controls. 10 μg of total RNA were used in each sample. All cerebellar ages contained CSF-1 and c-*fms* mRNA. CSF-1 was faintly visible in cortex after long exposures. For different samples, different exposure times were used, based on actin bands, to standardize for amount of mRNA. (B) (bottom) Expression of c-*fms* in neonate, P15, and adult hippocampus (1-3), and neonate, P15, and adult striatum (4-6); CSF-1 in neonate, P15, and adult hippocampus (8-10), and neonate and adult striatum (11-12). Lanes 7 and 13 contain corresponding yeast tRNA negative controls. 10 μg of total RNA were used in each sample. CSF-1 is not detectable at any age in either hippocampus or striatum. c-*fms* mRNA is present in all hippocampal and striatal samples with peaks at P15 in both.

form of CSF-1, while the 3.0 and 1.6 kb transcripts encode the membrane-bound form of CSF-1, both of which are biologically active. RT-PCR analysis revealed that the 4.6 and 2.3 kb transcripts were present in developing brain, at both E16 and P8 (Fig. 6A). In contrast, the two transcripts encoding the membrane-bound form were not detected at either age. These results were confirmed by Southern analysis of the PCR products; even with long exposure, no signal was detected in brain for the 3.0 and 1.6 kb transcripts (Fig. 6B). Thus, the mRNA encoding only the soluble growth factor, and not the membrane-bound form, is expressed in brain (Table 2).

Surface evoked potentials in *op/op* mice

The effects of CSF-1 on neural cultures and the expression of both the factor and its receptor in developing brain suggested a possible role for CSF-1 in neural development. The potential role of CSF-1 in brain development was explored by utilizing *op/op* mice, mutants that fail to synthesize any functional CSF-

Table 1. Regional expression of CSF-1 and CSF-1R mRNA during brain development

	E16	Neonate	P15	Adult
CSF-1				
Whole brain	+	+	+	+
Hippocampus	NA	–	–	–
Striatum	NA	–	–	–
Cerebellum	++	++	++	++
Cortex	+	+	+	+
CSF-1R				
Whole brain	+	+	++	+
Hippocampus	NA	+	++	+
Striatum	NA	+	++	+
Cerebellum	+	+	++	++
Cortex	+	+	++	++

Table is based upon semi-quantitative protection assays in Figs 4 and 5. NA, not assayed; –, no expression; +, low levels of expression; ++, readily detectable expression; CSF-1R, CSF-1 receptor.

1. Electrophysiologic recordings from the CNS of *op/op* mice were performed to ascertain whether any functional deficits were present in these animals. Fig. 7 illustrates representative brainstem auditory evoked potentials (BAEPs) and visual evoked potentials (VEPs) recorded from the scalp of a +/+ and an *op/op* mouse. The BAEP in the +/+ mouse consisted of 4-5 components, with an onset of Wave I at approximately 1.1 msec. The response was delayed and diminished in *op/op* mice, characterized by an absolute delay in the wave I latency, prolongation of the wave I-V interval, and a relative loss of the amplitude and integrity of the later components. A robust surface VEP was detected in all +/+ mice tested; in comparison, the response was poorly formed or absent in all six of the *op/op* mice examined.

Intracortical recordings of VEPs

A series of intracranial penetrations was undertaken to clarify the electrophysiologic abnormalities detected in *op/op* mice. VEPs were recorded from multiple cortical laminae within primary visual cortex, and an estimate of transmembrane current was made. Fig. 8 compares net intracortical transmembrane current flow in 6 control and 6 *op/op* mice. Total intracortical current was significantly reduced ($P<0.01$) in the *op/op* mice beginning at approximately 40 msec and continuing through 80 msecs. However, the onset latencies of current flow were coincident in the two groups, suggesting that the timing of retinal response and subcortical transmission was relatively unaffected in the *op/op* phenotype. The reduction in intracortical current flow is consistent with the poorly formed and diminished scalp-recorded VEPs.

Table 2. CSF-1 mRNA splice variants and their expression in developing brain

Transcript	Exon 6	Exon 9	Exon 10	Secreted	Uterus	Brain
4.6 kb	+	–	+	+	+	+
3.0 kb	–	–	+	–	+	–
2.3 kb	+	+	–	+	+	+
1.6 kb	–	+	–	–	+	–

The four mouse splice variants of CSF-1 mRNA are described. Uterine and brain expression is based on RT-PCR from Fig. 6. Only mRNAs containing exon 6, the secreted forms, are expressed in brain, whereas all splice variants are expressed in gravid uterus.

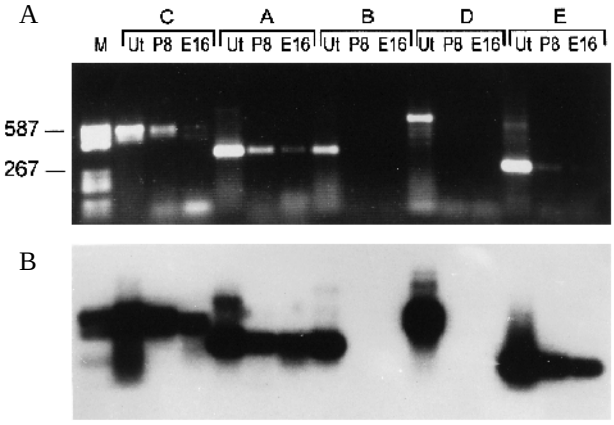

Fig. 6. RT-PCR analysis of CSF-1 mRNA splice variants in brain. (A) Ethidium-bromide stained gel of PCR products. Primer pairs A,B,C,D, and E refer to those outlined in Materials and Methods. Ut, day 14 pregnant uterus; E16 and P8 refer to brain samples from those ages. Appropriate size bands for each set of reactions are seen in uterus. However, only primer pairs C, A and E amplify cDNA from brain. M, DNA molecular weight marker V (Boehringer Mannheim). (B) Southern analysis of same gel. No amplification from brain is observed with primer pairs B and D. Hybridization to some bands of marker is seen due to plasmid sequences present in the probe. Autoradiogram represents a one hour exposure.

Grand average multiple unit activity (MUA) confirmed that the afferent volley reached visual cortex within normal latency limits in the *op/op* mice and documented a pattern of altered neural firing (Fig. 8B). In controls, the initial postsynaptic cortical activity represented net depolarization, reflected by a well-defined current sink in the central cortical laminae (not illustrated) and an associated excitatory burst of MUA. These responses were rapidly inhibited by current sources that drove the unit activity to baseline or below baseline levels by 90 msec (Fig. 8B). Both the initial excitation and the subsequent inhibition were reduced in the *op/op* mice. When expressed as a percentage, MUA in the *op/op* mice continued at levels greater than 25% of maximum for periods exceeding 190 msecs. These findings imply dysfunction in both excitatory and inhibitory cortical circuits.

Examination of GABAergic cortical circuitry in *op/op* mice

To explore possible alterations in intracortical circuitry, the $GABA_A$ antagonist bicuculline methiodide was microinjected into visual cortex of +/+ or *op/op* mice. Profiles of VEP, MUA and current source density (CSD) were compared before and after microinjection. In +/+ mice, bicuculline resulted in a sustained burst of excitatory MUA confined to the supragranular laminae (Fig. 9). This excitation followed the onset of cortical activity in lamina 4 by approximately 40 msec and was not associated with increased activity in thalamorecipient layers, thus clearly representing release of intracortical inhibition. The supragranular bursts achieved levels greater than 400 μV and represented local paroxysmal discharges. In contrast, equivalent volumes of bicuculline in *op/op* mice failed to produce the isolated, late supragranular

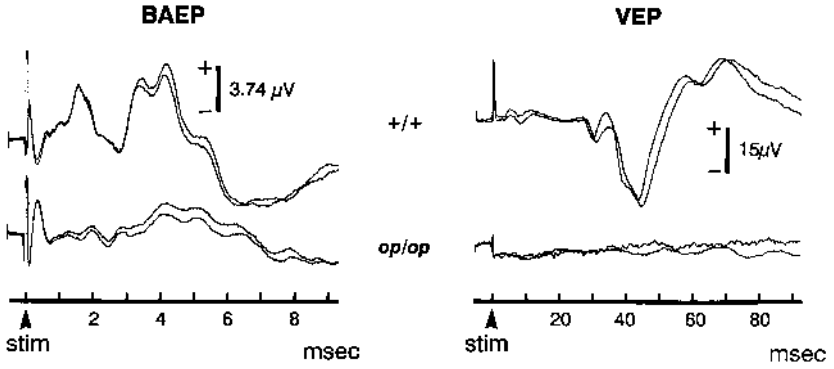

Fig. 7. Representative BAEPs and VEPs, recorded from scalp needle electrodes from anesthetized control versus *op/op* mice. Repeat trials are overlayed for each condition. BAEP latencies were prolonged and amplitudes reduced; VEP components were dramatically reduced or absent in the *op/op* mice.

activity. Rather, unit firing was diffusely elevated in several cortical laminae. These data indicate that elements of the normal cortical circuitry that balance excitation and inhibition and segregate responses to specific laminae are altered in the CSF-1-deficient mice.

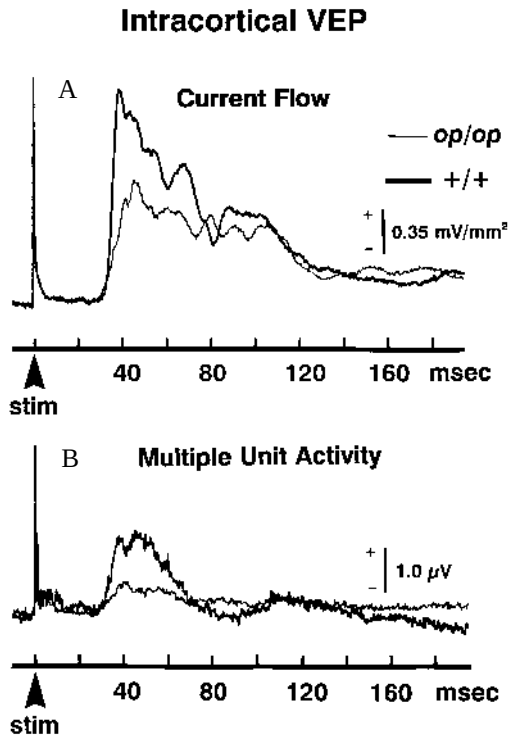

Fig. 8. (A) Net intracortical current flow evoked by high intensity, full-field flash stimulation. CSD was calculated from 14 sites, positioned to straddle the initial cortical dipole and separated by 100 μM. Each trace represents the grand mean of current flow data from 6 +/+ and 6 *op/op* mice. Prior to averaging, the CSD waveforms were full-wave rectified and summed across cortical sites to determine the absolute value of current flow at each time point evaluated (–10 to +190 msec). Note that the onset latency of current flow was coincident for each group. (B) MUA data, recorded simultaneously from the same sites as the above current flow measures. Each trace represents grand mean data from 6 +/+ and 6 *op/op* mice. The MUA trace prior to and immediately following stimulation represents the level of spontaneous unit firing in the sampled population. Note the increase in unit firing evident at 35-40 msec in both +/+ and *op/op* mice.

Treatment of *op/op* mice with exogenous CSF-1

To determine whether the electrophysiologic deficits in *op/op* mice could be ameliorated by growth factor replacement, the overall pattern of intracortical activity in a representative sample of *op/op* mice injected with CSF-1 was compared to the findings in saline-injected *op/op* littermates. Data from each hemisphere were scored separately by two observers who were blinded with respect to the status of the mice. Scoring of the field potentials from CSF-1 and saline-injected animals are shown in Table 3. In the CSF-1-treated mice, the electrophysiologic pattern fell within normal limits for 3 hemispheres (37.5%), another 3 were scored as mildly abnormal and 2 were considered moderately abnormal. In contrast, data in 5 hemispheres (62.5%) of saline-injected mice were scored as severely abnormal, and no data were considered either normal or mildly abnormal. Thus CSF-1 treatment partially but incompletely prevented development of the neural defects seen in *op/op* animals.

DISCUSSION

A role for CSF-1 in normal brain development has been implicated by the finding that *op/op* mice manifest neurologic abnormalities. Observation of these animals in a free-field cage setting suggested overt sensory deficits, since the mice failed to respond appropriately to simple stimuli (e.g. hand clapping). Scalp recordings of both BAEPs and VEPs demonstrated deficits consistent with diminished neurologic function in at least two sensory modalities. BAEPs provide a measure of the absolute timing and synchrony of afferent transmission in the myelinated auditory pathways extending from the cochlea to the medial geniculate nucleus (Legatt et al., 1988). The observed abnormality in the early components of this response in the *op/op* mouse suggests dysfunction in transduction and/or conduction in the distal portion of the sensory pathway. These results could partially reflect bone malformation affecting cranial nerve VIII. However, alterations observed in the amplitude and integrity of later BAEP components, and prolongation of the interval between waves I and V, suggest a primary neuronal abnormality.

Additional support for primary CNS neuronal deficits in *op/op* mice was obtained by multichannel intracortical recordings of the VEP. These studies documented a clear and consistent alteration in primary, secondary and tertiary processing of afferent information within visual cortex. The evidence for

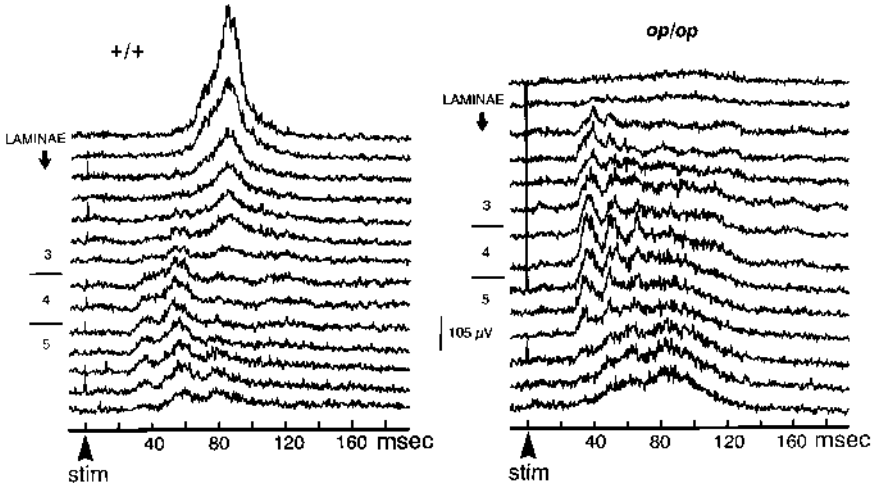

Fig. 9. Representative flash-evoked MUA following intracortical microinjection of the $GABA_A$ antagonist, bicuculline methiodide, in +/+ versus *op/op* mice. In the +/+, there is a very large burst of MUA confined to the supragranular laminae, which occurs at approximately 55 msec. This response becomes maximal by approximately 40 msec following the onset of initial cortical depolarization in lamina 4. In contrast, the *op/op* mice fail to show this late release of supragranular unit activity and instead display diffusely elevated activity across several cortical laminae.

a true neuronal deficit is compelling. (1) The initial evidence of altered intracortical function occurred with the earliest postsynaptic processing (i.e. 40 msec) and continued for more than 190 msec following flash stimulation. (2) Deficits were seen in both transmembrane current flow, a measure of graded postsynaptic responses, and MUA, an index of net ensemble action potentials (Vaughan and Arezzo, 1988). (3) Abnormal processing was evident in supragranular laminae as well as thalamorecipient layers, confirming altered intracortical circuitry. (4) The pattern of intracortical MUA, most notably the failure to effectively dampen the initial excitation, suggests alterations in inhibitory processing by cortical interneurons. Importantly, the timing of the presynaptic afferent volley reaching visual cortex was unaffected in the *op/op* mice, suggesting that elements of transduction and transmission in the retinal-striate pathways were intact and could not account for the observed deficits.

In concert, these electrophysiologic findings suggest a pattern of altered intracortical circuitry in the *op/op* mouse. Additional support for this concept was obtained by local microinfusion of the potent $GABA_A$ antagonist, bicuculline methiodide (Rose and Blakemore, 1974). In both the *op/op* and +/+ mouse, bicuculline clearly altered neural firing. However, in the +/+ mouse, the effect was principally limited to the supragranular laminae, resulting in a focal paroxysmal discharge, while responses in the *op/op* mouse were characterized by diffusely elevated unit firing in several laminae. The data are consistent with laminar alterations in the function of GABAergic inhibitory interneurons (for reviews, see Houser et al., 1984; Jones, 1988), although they do not directly address the mechanisms responsible for these abnormalities. These cells are intrinsic to the cortex and are activated relatively late, approximately 40 msec after the onset of cortical depolarization in the present study. They reflect fundamental elements of intracortical circuitry and determine the functional segregation of activity within cortical laminae (Kraut et al., 1990). Alterations in the functions of these interneurons, without substantial changes in earlier cortical elements, provide especially strong evidence for changes in local, intracortical neural processing in the *op/op* mouse.

Table 3. Electrophysiological pattern of intracortical activity in CSF-1-injected versus saline-injected *op/op* mice

	Within normal limits	Mildly abnormal	Moderately abnormal	Severely abnormal
op/op-CSF-1	XXX	XXX	XX	
op/op-saline			XXX	XXXXX

Data from each hemisphere were scored blindly with respect to the timing and pattern of laminar inversion, the integrity and temporal persistence of MUA, and the total pattern of current flow. Each X represents one hemisphere.

Although the electrophysiologic evidence of CNS abnormalities in *op/op* mice is compelling, the direct linkage of these changes in neural function to CSF-1 is less clear. To address this issue, *op/op* mice were treated from birth with injections of recombinant CSF-1, a manipulation that is known to reverse the osteopetrosis phenotype (Kodama et al., 1991; Wiktor-Jedrzejczak et al., 1991). The observation that the pattern of electrophysiologic abnormalities in *op/op* mice could be largely prevented by direct administration of CSF-1 provides strong evidence that the presence of CSF-1 directly influences neural development. This study also indicated that the influence of CSF-1 continues into the postnatal stage of neuronal maturation. The incompleteness of the rescue suggests that some irreversible deficits may occur during embryonic development.

Targeted deletion of genes that are normally expressed in CNS development often fails to cause histologic abnormalities in the brain. Such findings may suggest that enough overlap exists with similar proteins to prevent serious abnormalities in a single knockout. However, it is conceivable that abnormalities that cannot be detected by histochemical means are present in these animals. For example, cerebellar neurons from homozygous *src*⁻mutant mice, which have no detectable histologic abnormalities (Soriano et al., 1991), exhibited impaired neurite outgrowth in culture (Ignelzi et al., 1994). In the *op/op* mice, we similarly did not find anatomic or histopathological abnormalities; notably, there was no obvious change in glutamic acid decarboxylase (GAD), calbindin, synapsin or neurofilament immunohistochemistry in cortex (S. Walkley and J. A. K., data not shown). Other groups studying the brains of *op/op* mice have similarly failed to detect anatomic abnor-

malities (Chang et al., 1994). However, examination of the functional role of CSF-1 with electrophysiologic measures of sensory conduction and cortical processing has made it clear that abnormalities do exist. Such electrophysiologic techniques offer a sensitive method of detecting functional abnormalities in the absence of obvious anatomic defects and are likely to become an increasingly important method for evaluating functional consequences of gene mutation.

If CSF-1 is important in brain development, both CSF-1 and CSF-1R must be expressed at appropriate times in vivo in the CNS. Previous studies have demonstrated expression of CSF-1 in vivo in developing and adult whole brain (Bartocci et al., 1986; Rajavishisth et al., 1987; Thery et al., 1990; Burns et al., 1993). We examined its regional expression in developing brain and found the highest levels of CSF-1 mRNA in the cerebellum, with lower levels in cerebral cortex. In hippocampus and striatum, no CSF-1 mRNA was detected. Even more intriguing was the mRNA splice variant expression. We found that the CSF-1 mRNAs encoding only the secreted form of the growth factor, and not the mRNAs encoding the membrane-bound form, were transcribed in brain. The regional variation in, and specific splice variant expression of, CSF-1 in the developing CNS suggest that it is not released as a non-specific immune mediator, but rather subserves a precise trophic role in particular developing brain regions. CSF-1R mRNA was expressed in developing brain as well, with increasing expression through development, peaking postnatally before declining in the adult. The normal expression of CSF-1 and CSF-1R mRNA in cortex during development is consistent with the observed deficit in *op*/*op* cortical function.

Additional clues to the physiologic role of CSF-1 come from its effects on neural cells in vitro. To some extent, CSF-1 enhances the survival of neurons in embryonic brain cultures at physiologic doses of CSF-1 (see Stanley et al., 1983 for discussion of physiologic levels of CSF-1). However, the more dramatic effect of CSF-1 treatment is on process outgrowth by developing neurons. In serum-free, low-density conditions, untreated cultures exhibit essentially no process outgrowth. In contrast, addition of physiologic doses of CSF-1 results in neurite outgrowth by most cells, with more than 90% of cells from cortex, and nearly 80% of cerebellar cells, exhibiting processes. The fact that these two regions exhibit the greatest degree of neurite outgrowth is consistent with expression data showing CSF-1 mRNA in cortex and cerebellum. Thus, even though glial cells throughout brain probably express CSF-1R, particular regions of brain, which contain CSF-1 in vivo, in development respond most impressively to exogenous treatment with CSF-1 in vitro. The combination of these findings presents a strong case for a physiologic role of CSF-1 in process outgrowth.

Neural cells cultured from *op/op* mice exhibit the same survival response as +/+ neural cells in response to CSF-1. Interestingly, we found that the effect of CSF-1 on process outgrowth was significantly decreased in *op/op* cultures in two ways: first, there was a lag time in *op/op* cultures for process extension, with a smaller percentage of process-bearing cells at days 1 and 2 after plating; second, the complexity of the processes was decreased in *op/op* cultures as assessed by the length of neurites and the number of branch points. These observations indicate an impaired response to CSF-1, the basis of which is unknown. Brain microglia may be quantitatively decreased in *op/op* mice, since fewer microglia are present in retina during development (Cecchini et al., 1994). Alternatively, microglia may be qualitatively altered by the absence of CSF-1, resulting in an altered pattern of cytokine response and/or expression.

The mechanism of CSF-1 activity has not been determined. Its neurotrophic effects are probably indirect, mediated by microglial cells. Microglia are known to express surface CSF-1R, and c-*fms* mRNA is detectable in macrophage-like cells from astroglial cultures (Sawada et al., 1990; Hao et al., 1990). Cultured brain microglia proliferate in response to CSF-1 and exhibit marked morphological changes (Sawada et al., 1990; Suzumura et al., 1990). In contrast, c-*fms* is not expressed by cultured cortical neurons. The predominant neural cell type expressing CSF-1R almost certainly is microglia in vivo as well (Cecchini et al., 1994). Additionally, in single cell cultures, CSF-1 was unable to support the survival of neurons (data not shown), further suggesting, although not proving, that the effects of CSF-1 on neurons are mediated by glial cells.

CSF-1 was initially characterized as a hematopoietic growth factor specific for cells of the mononuclear phagocyte lineage (Stanley et al., 1983). Subsequently, a role in fertility was identified (Pollard et al., 1987; Arceci et al., 1989; Regenstreif and Rossant, 1989; Pollard et al., 1991). Consistent with these roles, homozygous *op/op* mice are deficient in monocytes and macrophages and display impaired fertility (Wiktor-Jedrzejczak et al., 1990; Pollard et al., 1991). The data presented here suggest that CSF-1 is also an important factor in CNS development. CSF-1 treatment of neural cultures increases the number and differentiation of neurons relative to untreated cultures, and both CSF-1 and CSF-1R mRNA are expressed in vivo in developing brain. Homozygous *op/op* mice display alterations in intracortical circuitry that cause deficiencies in vision, and these can be prevented with daily CSF-1 treatment. These results implicate CSF-1 as an important growth factor in normal mouse brain development.

We thank F.-C. Chuan, S. Seto, and M.S. Litwak for providing excellent technical assistance. We also thank Steve Clark and Genetics Institute for providing human CSF-1. Our gratitude is extended to Dr David K. Batter for critical reading of the manuscript. This work was supported by a grant from the Muscular Dystrophy Association (to M.F.M.), by Irma T. Hirschl/Monique-Weill Caulier Career Scientist Awards (to M. F. M. and J. W. P.), by American Cancer Society grant DB-28 (to J. W. P.), and by NIH grants HD30280 (to J. W. P.), NS20013 and NS20778 (to J. A. K.). M. D. M. was supported (in part) by NIH MSTP Training Grant T32GM07288.

REFERENCES

Arceci, R. J., Shanahan, F., Stanley, E. R. and Pollard, J. W. (1989). Temporal expression and location of colony stimulating factor-1 (CSF-1) and its receptor in the female reproductive tract are consistent with CSF-1 regulated placental development. *Proc. Natl. Acad. Sci. USA* **86**, 8818-8822.

Bartocci, A., Pollard, J. W. and Stanley, E. R. (1986). Regulation of colony-stimulating factor-1 during pregnancy. *J. Exp. Med.* **164**, 956-961.

Begg, S. K., Radley, J. M., Pollard, J. W., Chisholm, O. T., Stanley, E. R. and Bertoncello, I. (1993). Delayed hematopoietic development in osteopetrotic (op/op) mice. *J. Exp. Med.* **177**, 237-242.

Brosnan, C. F., Shafit-Zagardo, B., Aquino, D. A. and Berman, J. W. (1993). Expression of monocyte/macrophage growth factors and receptors in the central nervous system. *Adv. Neurol.* **59**, 349-361.

Burns, T. M., Clough, J. A., Klein, R. M., Wood, G. W. and Berman, N. E. J. (1993). Developmental regulation of cytokine expression in the mouse brain. *Growth Factors* **9**, 253-258.

Cecchini, M. G., Dominguez, M. G., Mocci, S., Wetterwald, A., Felix, R., Fleisch, H., Chisholm, O., Hofstetter, W., Pollard, J. W. and Stanley, E. R. (1994). Role of colony stimulating factor-1 in the establishment and regulation of tissue macrophages during postnatal development of the mouse. *Development* **120**, 1357-1372.

Chang, Y., Albright, S. and Lee, F. (1994). Cytokines in the central nervous system: expression of macrophage colony stimulating factor and its receptor during development. *J. Neuroimm.* **52**, 9-17.

Chomczynski, P. and Sacchi, N. (1987). Single-step method of RNA isolation by guanidinium-thiocyanate-phenol-chloroform extraction. *Ann. Biochem.* **162**, 156-158.

Cohen, P. E., Arceci, R. J., Chisholm,O., Stanley, E. R., and Pollard, J. W. (1996). Absence of colony stimulating factor-1 in osteopetrotic mice results in male fertility defects. *Biol. Reprod.*, in press.

Daiter, E., Pampfer, S., Yeung, Y. G., Barad, D., Stanley, E. R. and Pollard, J. W. (1992). Expression of colony stimulating factor-1 in the human uterus and placenta. *J. Clin. Endo. Metab.* **74**, 850-858.

Freeman, J. A. and Nicholson, C. (1975). Experimental optimization of current source density technique for anuran cerebellum. *J. Neurophysiol.* **38**, 369-382.

Givre, S. J., Schroeder, C. E. and Arezzo, J. C. (1994). Contribution of extrastriate area V4 to the surface-recorded flash VEP in the awake macaque. *Vision Res.* **34**, 415-428.

Hao, C., Guilbert, L. J. and Federoff, S. (1990). Production of colony-stimulating factor-1 (CSF-1) by mouse astroglia in vitro. *J. Neurosci. Res.* **27**, 314-323.

Houser, C. R., Vaughan, J. E., Hendry, S. H. C., Jones, E. G. and Peters, A. (1984). GABA neurons in the cerebral cortex. In *Cerebral Cortex* (ed. E. G. Jones and A. Peters). pp. 63-89. New York: Plenum Press.

Ignelzi, M. A., Jr., Miller, D. R., Soriano, P. and Maness, P. F. (1994). Impaired neurite outgrowth of src-minus cerebellar neurons on the cell adhesion molecule L1. *Neuron* **12**, 873-884.

Jones, E. G. (1988). GABA neurons and their cotransmitters in the primate cerebral cortex. In *Neurotransmitters and Cortical Function from Molecules to Mind* (ed. M. Avoli, T. A. Reader, R. W. Dykes and P. Gloor). pp. 125-152. New York: Plenum Press.

Kawasaki, E. S. and Ladner, M. B. (1990). Molecular biology of macrophage colony-stimulating factor. In *Colony-Stimulating Factors, Molecular and Cellular Biology* (ed. T. M. Dexter, J. M. Garland and N. G. Testa). pp. 155-176. New York: Marcei Dekker, Inc.

Kodama, H., Yamasaki, A., Nose, M., Niida, S., Ohgame, Y., Abe, M., Kumegawa, M. and Suda, T. (1991). Congenital osteoclast deficiency in osteopetrotic (op/op) mice is cured by injections of macrophage colony-stimulating factor. *J. Exp. Med.* **173**, 269-272.

Kraut, M. A., Arezzo, J. C. and Vaughan, H. G., Jr. (1990). Inhibitory processes in the flash evoked potential of the monkey. *Electroenceph. Clin. Neurophys.* **76**, 440-452.

Ladner, M. B., Martin, G. A., Noble, J. A., Wittman, V. P., Warren, M. K., McGrogan, M. and Stanley, E. R. (1988). cDNA cloning and expression of murine macrophage colony-stimulating factor from L929 cells. *Proc. Natl. Acad. Sci. USA* **85**, 6706-6710.

Legatt, A. D., Arezzo, J. C. and Vaughan, H. G., Jr (1988). The anatomic and physiologic bases of brain stem auditory evoked potentials. In *Neurol Clinics*, Vol. 6, No. 4. (ed. R. Gilmore) pp. 681-704. Philadelphia: W. B. Saunders Company.

Ludlam, W. H., Zang, Z., McCarson, K. E., Krause, J. E., Spray, D. C. and Kessler, J. A. (1994). mRNAs encoding muscarinic and substance P receptors in cultured sympathetic neurons are differentially regulated by LIF or CNTF. *Dev. Biol.* **164**, 528-539.

Marks, S. C., Jr. and Lane, P. W. (1976). Osteopetrosis, a new recessive skeletal mutation on chromosome 12 of the mouse. *J. Heredity* **67**, 11-18.

Mehler, M. F., Rozental., R., Dougherty, M., Spray, D. C. and Kessler, J. A. (1993). Cytokine regulation of neuronal differentiation of hippocampal progenitor cells. *Nature* **362**, 62-65.

Pampfer, S., Daiter, E., Barad, D. and Pollard, J. W. (1992). Expression of the colony-stimulating factor-1 receptor (c-fms proto-oncogene product) in the human uterus and placenta. *Biol. Reprod.* **46**, 48-57.

Pollard, J. W., Bartocci, A., Arceci, R., Orlofsky, A., Ladner, M. B. and Stanley, E. R. (1987). Apparent role of the macrophage growth factor, CSF-1, in placental development. *Nature* **330**, 484-486.

Pollard, J. W., Hunt, J. W., Wiktor-Jedrzejczak, W. and Stanley, E. R. (1991). A pregnancy defect in the osteopetrotic (op/op) mouse demonstrates the requirement for CSF-1 in female fertility. *Dev. Biol.* **148**, 273-283.

Pollard, J. W. and Stanley, E. R. (1996). Pleiotropic roles for CSF-1 in development defined by the mouse mutant osteopetrotic (op). *Adv. Dev. Biochem.* **4**, 153-193.

Price, L. K. H., Choi, H. U., Rosenberg, L. and Stanley, E. R. (1992). The predominant form of secreted colony stimulating factor-1 is a proteoglycan. *J. Biol. Chem.* **267**, 2190-2199.

Rajavishisth, T. B., Eng, R., Shadduck, R. K., Waheed, A., Ben-Avram, C. M., Shively, J. E. and Lusis, A. J. (1987). Cloning and tissue-specific expression of mouse macrophage colony-stimulating factor mRNA. *Proc. Natl. Acad. Sci. USA* **84**, 1157-1161.

Regenstreif, L. J. and Rossant, J. (1989). Expression of the c-fms proto-oncogene and of the cytokine, CSF-1, during mouse embryogenesis. *Dev. Biol.* **133**, 284-294.

Rose, D. and Blakemore, C. (1974). Effects of bicuculline on functions of inhibition in visual cortex. *Nature* **249**, 375-377.

Roth, P. and Stanley, E. R. (1992). The biology of CSF-1 and its receptor. *Curr. Top. Microbiol. Immunol.* 141-167.

Sawada, M., Suzumura, A., Yamamoto, H. and Marunouchi, T. (1990). Activation and proliferation of the isolated microglia by colony stimulating factor-1 and possible involvement of protein kinase C. *Brain Res.* **509**, 119-124.

Soriano, P., Montgomery, C., Geske, R. and Bradley, A. (1991). Targeted disruption of the c-src proto-oncogene leads to osteopetrosis in mice. *Cell* **64**, 693-702.

Stanley, E. R., Guilbert, L. J., Tushinski, R. J. and Bartelmez, S. H. (1983). CSF-1-a mononuclear phagocyte lineage specific haemopoietic growth factor. *J. Cell. Biochem.* **21**, 151-159.

Suzumura, A., Sawada, M., Yamamoto, H. and Marunouchi, T. (1990). Effects of colony stimulating factors on isolated microglia in vitro. *J. Neuroimm.* **30**, 111-120.

Thery, C., Hetier, E., Evrard, C. and Mallat, M. (1990). Expression of macrophage colony-stimulating factor gene in the mouse brain during development. *J. Neurosci. Res.* **26**, 129-133.

Vaughan, H. G., Jr and Arezzo, J. C. (1988). The neural basis of event-related potentials. In *Human Event-Related Potentials*, EEG Handbook, Vol. 3 (ed. T. W. Picton), pp. 45-96. Amsterdam: Elsevier Scientific Publishers.

Wiktor-Jedrzejczak, W., Ahmed, A., Szczylik, C. and Skelly, R. R. (1982). Hematological characterization of congenital osteopetrosis in op/op mouse. *J. Exp. Med.* **156**, 1516-1527.

Wiktor-Jedrzejczak, W., Bartocci, A., Ferrante, A. W., Jr., Ahmed-Ansari, A., Sell, K. W., Pollard, J. W. and Stanley, E. R. (1990). Total absence of colony-stimulating factor 1 in the macrophage-deficient osteopetrotic (op/op) mouse. *Proc. Natl. Acad. Sci. USA* **87**, 4828-4832.

Wiktor-Jedrzejczak, W., Urbanowska, E., Aukerman, S. L., Pollard, J. W., Stanley, E. R., Ralph, P., Ansari, A. A., Sell, K. W. and Szperl, M. (1991). Correction by CSF-1 of defects in the osteopetrotic op/op mouse suggests local., developmental., and humoral requirements for this growth factor. *Exp. Hematol.* **19**, 1049-1054.

Witmer-Pack, M. D., Hughes, D. A., Schuler, G., Lawson, L., McWilliam, A., Inaba, K., Steinman, R. and Gordon, S. (1993). Identification of macrophages and dendritic cells in the osteopetrotic (op/op) mouse. *J. Cell Sci.* **104**, 1021-1029.

Yoshida, H., Hayashi, S., Kunisada, T., Ogawa, M., Nishikawa, S., Okamura, H., Sudo, T., Shultz, L. D. and Nishikawa, S. (1990). The murine mutation osteopetrosis is in the coding region of the macrophage colony stimulating factor gene. *Nature* **345**, 442-443.

(Accepted 5 June 1996)